Neutrino Oscillations with LSND

Ion Stancu [a] *

[a]Department of Physics, University of California, Riverside, CA 92521, USA
E-mail: ion.stancu@ucr.edu

The Liquid Scintillator Neutrino Detector (LSND) at the Los Alamos Meson Physics Facility (LAMPF) has conducted searches for $\bar{\nu}_\mu \to \bar{\nu}_e$ oscillations using $\bar{\nu}_\mu$ from μ^+ decay at rest (DAR) and for $\nu_\mu \to \nu_e$ oscillations using ν_μ from π^+ decay in flight (DIF). For the 1993-1995 data taking period, significant beam-excess events have been found in both oscillation channels. For the DAR search, a total excess of $51.8^{+18.7}_{-16.9} \pm 8.0$ events from the $\bar{\nu}_e\, p \to e^+\, n$ inverse β-decay reaction is observed, with e^+ energies between 20–60 MeV. For the DIF search, a total excess of $18.1 \pm 6.6 \pm 4.0$ events from the $\nu_e\, C \to e^-\, X$ inclusive reaction is observed, with e^- energies between 60–200 MeV. If interpreted as neutrino oscillations, these excesses correspond to oscillation probabilities of $(3.1 \pm 1.2 \pm 0.5) \times 10^{-3}$ and $(2.6 \pm 1.0 \pm 0.5) \times 10^{-3}$, respectively. Additional data collected during the 1996-1998 runs has been preliminarily analyzed for the DAR channel and yields very good agreement with the previously obtained results, for a combined oscillation probability of $(3.3 \pm 0.9 \pm 0.5) \times 10^{-3}$.

1. INTRODUCTION

In the past years, a considerable number of experiments have searched for neutrino oscillations, where a neutrino of one type (say $\bar{\nu}_\mu$) spontaneously transforms into a neutrino of another type (say $\bar{\nu}_e$). For this phenomenon to occur, neutrinos must be massive and the lepton number conservation law must be violated. In 1995 the LSND experiment published data showing candidate events that are consistent with $\bar{\nu}_\mu \to \bar{\nu}_e$ oscillations [2]. Additional data are reported here that provide stronger evidence for neutrino oscillations in this channel [3]. Further supporting evidence is provided by the signal in the $\nu_\mu \to \nu_e$ charge-conjugate channel [4]. The two oscillations searches have completely different neutrino fluxes, backgrounds, and systematics from each other.

2. NEUTRINO SOURCE AND DETECTOR

The primary source of neutrinos for this experiment is the 30-cm long A6 water target located at approximately 30 m from the detector center. About 3.4% of the π^+ produced in this target decay in flight before reaching the water-cooled copper beam stop, generating a ν_μ flux with energies up to 300 MeV – illustrated in Fig. 1. Two upstream carbon targets, A1 and A2, located approximately 135 m and 110 m, respectively, from the detector center also contribute to the ν_μ DIF flux – as indicated in Fig. 1. The remaining π^+ stop and decay in the beam dump, producing the DAR $\bar{\nu}_\mu$ flux through the $\pi^+ \to \mu^+ \nu_\mu$ decay, followed by $\mu^+ \to e^+ \nu_e \bar{\nu}_\mu$, with an endpoint energy of 52.8 MeV – illustrated in Fig. 2. The systematic errors are calculated to be 15% for the DIF flux and 7% for the DAR flux, as confirmed by our measurements of the $\nu_\mu\, C \to \mu^-\, {}^{12}N_{gs}$ and $\nu_e\, C \to e^-\, {}^{12}N_{gs}$ exclusive reactions [5,6], respectively. The data discussed here corresponds to 14772 Coulombs of 800 MeV protons at the primary beam stop during the years 1993-1995. *Preliminary* results that include the 1996-1998 runs are also presented for the DAR data, corresponding to an additional 14470 Coulombs of protons on target (POT). During these runs, the water target at A6 was replaced by a high-Z target configuration for the APT project. Consequently, the DAR and DIF fluxes were reduced to approximately 66% and 51%, respectively, from the original fluxes.

The LSND apparatus is described in detail elsewhere [7]. Briefly, it consists of a steel tank filled

*Representing the LSND Collaboration [1]

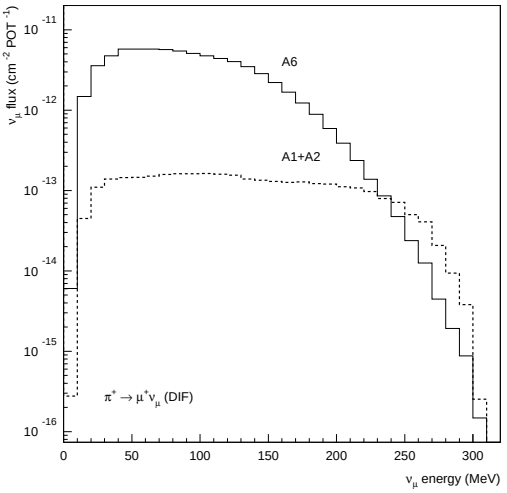

Figure 1. Calculated ν_μ DIF flux at the detector center from the A6 target (solid histogram) and from the A1+A2 targets (dashed histogram).

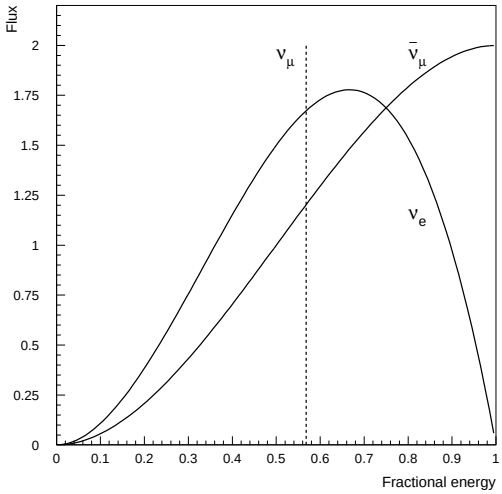

Figure 2. Flux shape of neutrinos from pion and muon decay at rest as a function of the fractional energy ($E_{max} = 52.8$ MeV).

with 167 metric tons of liquid scintillator (mineral oil – CH_2 – doped with 0.031 g/l of butyl-PBD) and viewed by 1220 8-inch photo-multiplier tubes (PMTs). This configuration allows one to perform not only position and direction Čerenkov imaging, but also calorimetry – with an energy resolution of 6.6% at the Michel spectrum endpoint. The standard reconstruction algorithm provides a spatial resolution of about 25 cm and a direction accuracy of approximately 12° for electron events in the Michel energy range. A veto shield viewed by 292 5-inch PMTs surrounds the detector, providing both passive and active shielding. Additional passive shielding is provided by about 9 m of Fe-equivalent between the beam stop and the detector, as well as by 2 kg/cm^2 of overburden on top of the detector tunnel.

3. THE DECAY-AT-REST ANALYSIS

The DAR $\bar{\nu}_e$ candidate events are identified through the inverse β-decay reaction, $\bar{\nu}_e\, p \to e^+\, n$. Thus, the detection signature consists of a positron and a space-time correlated 2.2 MeV photon, from the neutron capture on free protons ($n\, p \to d\, \gamma$). This two-fold signature provides a unique and powerful $\bar{\nu}_e$ appearance identification and, at the same time, a relatively low level of background – dominated by the intrinsic $\bar{\nu}_e$ contamination in the beam.

Particle identification (PID) for this analysis is achieved through a PID parameter that relies on the quality of the position, timing and angle fit [3]. The positrons are required to have $36 < E_e < 60$ MeV, be reconstructed within the 35 cm fiducial volume, and have less than 4 hits in the veto shield. The lower energy limit is dictated by the endpoint energy of the $\nu_e\, C \to e^-\, X$ charged-current reaction, whereas the upper limit is simply determined by Michel spectrum endpoint. A likelihood ratio, R, is employed to determine whether a γ is a 2.2 MeV photon correlated with the positron, or is from an accidental coincidence. R depends on the time difference between the positron and the γ, the tank hit multiplicity

for the γ, and the reconstructed distance between the positron and the γ, as shown in Fig. 3.

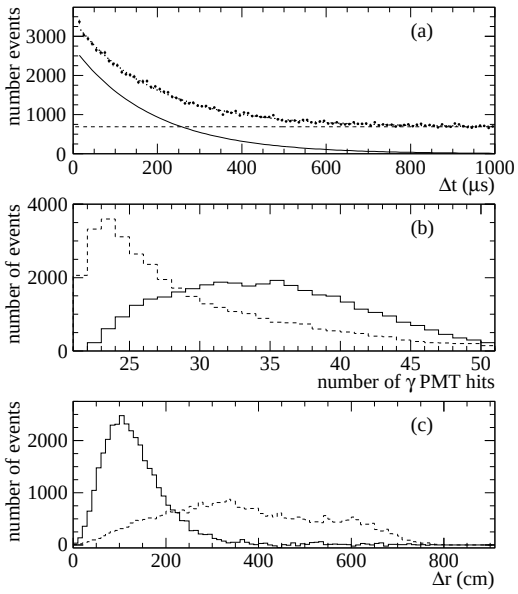

Figure 3. (a) Time difference between the gamma and the primary event, (b) gamma tank hit multiplicity distribution, and (c) reconstructed distance between the gamma and the primary event for correlated 2.2 MeV gammas (solid histograms) and for accidental gammas (dashed histograms).

Using very stringent selection criteria for the identification of the e^+ with correlated 2.2 MeV gammas yields 22 events with e^+ energy between 36 and 60 MeV and only 4.6 ± 0.6 background events (2.5 beam-unrelated and 2.1 beam-related background events). The probability that the excess is entirely due to a statistical fluctuation is 4.1×10^{-8}.

This very tight set of selection criteria establishes the presence of a significant beam-induced $\bar{\nu}_e$ excess events. However, in order to obtain an accurate measure of the $\bar{\nu}_e$ excess, the entire beam-excess R distribution of the $\bar{\nu}_e$ sample is fitted. The power of this procedure has been demonstrated using the $\nu_\mu\, C \rightarrow \mu^-\, X$ and $\nu_e\, C \rightarrow e^-\, {}^{12}N_{gs}$ samples [5,6]. At the same time, the lower energy limit is relaxed from 36 to 20 MeV, as there are no physical processes that produce an electron with a correlated 2.2 MeV gamma above 20 MeV. After subtracting the beam-induced neutrino background there is a total excess of $51.8^{+18.7}_{-16.9} \pm 8.0$ events which, if interpreted as neutrino oscillations, corresponds to an oscillation probability of $(3.1 \pm 1.2 \pm 0.5) \times 10^{-3}$. If the observed excess is due to neutrino oscillations, Fig. 4 shows the allowed region (90% and 99% likelihood regions) in the $(\sin^2 2\theta, \Delta m^2)$ mixing space, as determined from a maximum likelihood fit to the L/E distribution of the entire data sample.

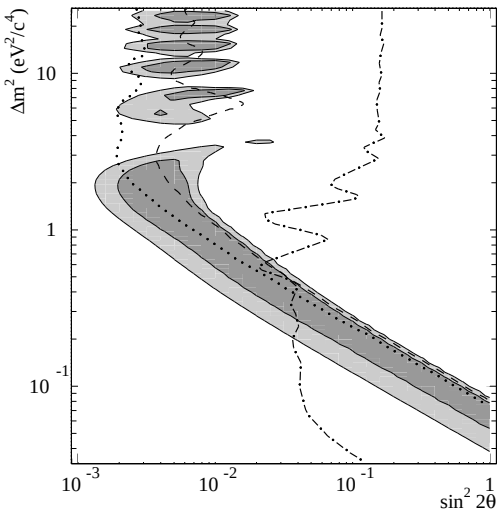

Figure 4. The LSND allowed regions (90% and 99% likelihood regions) from the 1993-1995 DAR analysis. Also shown are the 90% CL limits from KARMEN-1 (dashed), BNL-E776 (dotted) and Bugey (dot-dashed).

Ten months of additional data have been collected during the 1996-1998 runs, with the water

Table 1
The LSND "gold-plated" DAR samples ($36 < E_e < 60$ MeV and $R > 30$) for the 1993-1995, 1996-1998, and 1993-1998 running periods. All numbers referring to the data collected after 1995 are *preliminary*.

Year	Beam On	Beam Off	Neutrino Background	Excess
1993-1995	22	2.5 ± 0.4	2.1 ± 0.4	17.4 ± 4.7
1996-1998	11	3.7 ± 0.4	1.2 ± 0.4	6.1 ± 3.4
1993-1998	33	6.2 ± 0.6	3.3 ± 0.6	23.5 ± 5.8

Table 2
Evolution of the number of DAR excess events and oscillation probabilities from fits to the R distribution. The electron energy is $20 < E_e < 60$ MeV for all periods, except for 1993-1994 when only the $36 < E_e < 60$ MeV has been fitted. All numbers referring to the data collected after 1995 are *preliminary*.

Year	Fitted XCS	Oscillations XCS	Oscillation Probability (%)
1993-1994	19.1 ± 9.3	16.4 ± 9.9	$0.34 \pm 0.19 \pm 0.07$
1993-1995	63.5 ± 20.0	51.2 ± 20.2	$0.31 \pm 0.12 \pm 0.05$
1993-1997	100.1 ± 23.4	82.8 ± 23.7	$0.31 \pm 0.09 \pm 0.05$
1993-1998	111.8 ± 23.8	90.0 ± 24.0	$0.33 \pm 0.09 \pm 0.05$

target replaced by a close-packed high-Z target for tritium production testing. The μ^+ DAR neutrino flux in this configuration is approximately $2/3$ of the neutrino flux with the original beam stop, while the π^+ DIF neutrino flux is reduced by a factor of two with respect to the original flux. *Preliminary* results from the 1996-1998 runs are given in Table 1, in which we list the total number of beam on, (rescaled) beam off, beam-related background and net excess events for the "gold-plated" sample, along with the corresponding results for the initial running period 1993-1995, as well as for the combined 1993-1998 data. Table 2 shows the evolution of the cumulative number of DAR excess events and oscillation probabilities from fits to the R distribution over different LSND running periods. The *preliminary* allowed regions in the $(\sin^2 2\theta, \Delta m^2)$ parameter space obtained from the DAR analysis of the entire 1993-1998 data are shown in Fig. 5. In addition to the previous limits from Bugey and BNL-E776, the results from the upgraded KARMEN-2 experiment are also shown [8]. The net event excess observed in the DAR channel has constantly gained significance over the different running periods of LSND, and the resulting oscillation probabilities have remained consistent, within the statistics of the experiment.

4. THE DECAY-IN-FLIGHT ANALYSIS

Candidate events for $\nu_\mu \to \nu_e$ oscillation from the DIF ν_μ flux consist of a single, isolated electron in the energy range 60–200 MeV. Similarly to the DAR analysis, events are required to have less than 4 hits in the veto shield, and reconstruct within the 35 cm fiducial volume. Past and future space-time correlations are used to reduce the cosmic ray muon-related background. The electron PID is now based on an entirely new event reconstruction, which relies on a maximal charge and timing likelihood approach. The essential components of electron PID are the differences in timing characteristic of the components of light produced in an event: scintillation, and Čerenkov light, both direct and rescattered. The event likelihood fitting returns PID parameters based on the fraction of Čerenkov light in the event, and the PMT time likelihoods for scintillation and Čerenkov light. This new algorithm im-

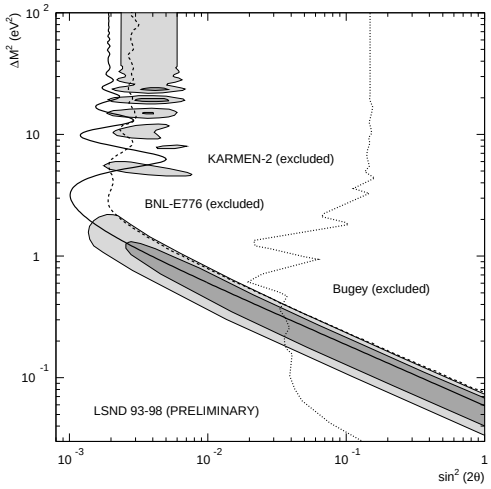

Figure 5. The *preliminary* LSND allowed regions in the $(\sin^2 2\theta, \Delta m^2)$ space from the 1993-1998 data. In addition to the previous limits from Bugey and BNL-E776, the current limit from KARMEN-2 is also shown.

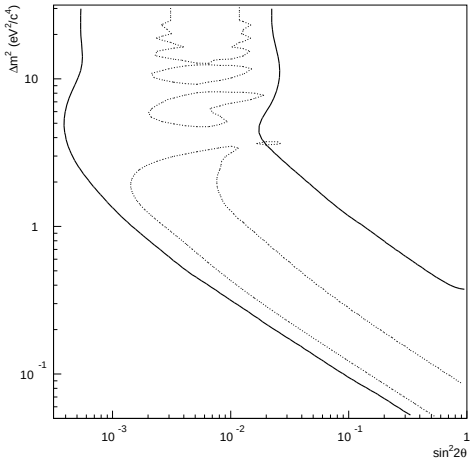

Figure 6. The 95% confidence level region (solid contours) for the 1993-1995 LSND $\nu_\mu \to \nu_e$ DIF analysis, along with the favoured regions from the DAR measurement for the same running period.

proves the position and direction accuracy by a factor of two over that obtained with the standard reconstruction. The spatial position resolution is now approximately 11 cm and the angle resolution is approximately 6° for electron events over the energy interval of interest for this analysis.

Using two independent analyses [4], a total of 40 beam-on events and 175 beam-off events are observed, corresponding to a beam-induced excess of 27.7 ± 6.4 events. The neutrino-induced backgrounds are dominated by $\mu^+ \to e^+ \bar{\nu}_\mu \nu_e$ and $\pi^+ \to e^+ \nu_e$ decays in flight in the A6 beam stop area, and are calculated to be 9.6 ± 1.9 events. Therefore, a total excess of $18.1 \pm 6.6 \pm 4.0$ events is observed above the expected background from conventional processes. The excess events are consistent with $\nu_\mu \to \nu_e$ oscillations with an oscillation probability of $(2.6 \pm 1.0 \pm 0.5) \times 10^{-3}$. A fit to the event distributions yields the allowed region in the $(\sin^2 2\theta, \Delta m^2)$ parameter space shown in Fig. 6, which is consistent with the allowed region from the $\bar{\nu}_\mu \to \bar{\nu}_e$ DAR search.

5. CONCLUSIONS

In summary, the LSND experiment observes significant excess of events for both the $\bar{\nu}_\mu \to \bar{\nu}_e$ and $\nu_\mu \to \nu_e$ oscillation searches, corresponding to oscillation probabilities of $(3.3 \pm 0.9 \pm 0.5) \times 10^{-3}$ and $(2.6 \pm 1.0 \pm 0.5) \times 10^{-3}$, respectively. These two appearance searches have completely different neutrino fluxes, backgrounds, and systematics and together provide strong evidence for neutrino oscillations in the range of $0.2 < \Delta m^2 < 2.0$ eV^2.

The experiment has completed data taking in December 1998 and is currently being decomissioned in preparation for the MiniBooNE experiment at FermiLab [9]. Significant efforts are well underway to develop the global analysis tools for a combined DAR+DIF analysis with higher efficiencies and statistics for the entire 1993-1998 running period.

REFERENCES

1. The LSND collaboration consists of: E. D. Church, K. McIlhany, I. Stancu, W. Strossman, G. J. VanDalen (UC Riverside); W. Vernon (UC San Diego); D. O. Caldwell, S. Yellin (UC Santa Barbara); D. Smith, J. Waltz (Embry Riddle Aeronautical University); I. Cohen (Linfield College); R. L. Burman, J. B. Donahue, F. J. Federspiel, G. T. Garvey, W. C. Louis, G. B. Mills, V. Sandberg, R. Tayloe, D. H. White (Los Alamos National Laboratory); R. M. Gunasingha, R. Imlay, H. J. Kim, W. Metcalf, N. Wadia (Louisiana State University); A. Fazely (Southern University); C. Athanassopoulos, L. B. Auerbach, R. Majkic, D. Works, Y. Xiao (Temple University).
2. C. Athanassopoulos *et. al.* , Phys. Rev. Lett. **75**, 2650 (1995).
3. C. Athanassopoulos *et. al.* , Phys. Rev. C **54**, 2685 (1996).
4. C. Athanassopoulos *et. al.* , Phys. Rev. C **58**, 2489 (1998).
5. C. Athanassopoulos *et. al.* , Phys. Rev. C **56**, 2806 (1997).
6. C. Athanassopoulos *et. al.* , Phys. Rev. C **55**, 2078 (1997).
7. C. Athanassopoulos *et. al.* , Nucl. Instrum. Methods A **388**, 149 (1997).
8. T. Jannakos, *"Results from the KARMEN Experiment"*, these proceedings.
9. I. Stancu, *"The Future of the Short-Baseline Neutrino Oscillation Experiments in the US: MiniBooNE and ORLaND"*, these proceedings.